ChemComm

Accepted Manuscript

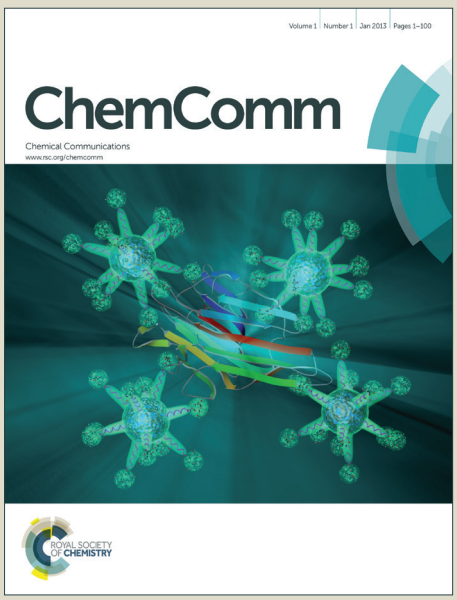

ROYAL SOCIETY OF CHEMISTRY

www.rsc.org/chemcomm

Journal Name

RSCPublishing

COMMUNICATION

Adjusting the inter-particle spacing of a nanoparticle array at sub-nanometre scale by thermal annealing

Cite this: DOI: 10.1039/xoxxoooooox

J. Zhou[a,d], H. Liu[b], T. Wang[a], Y. Li, J. Zhang[*,c], Z. Lu[*,b], Y. Fu[*,a] and F. Li[d]

Received ooth January 2012,
Accepted ooth January 2012

DOI: 10.1039/xoxxoooooox

www.rsc.org/

A successful attempt to fabricate nanoparticle arrays with sub-nanometre spacing by thermal annealing of the prepared nanoparticle self-assembly was made. The molecular dynamics simulation indicated the spacing decrease could be attributable to the temperature-enhanced mobility of the ligand, which promoted the relaxation of the nanoparticles to a more compact arrangement.

In a nanoparticle array, the spacing between two adjacent nanoparticles is crucial to their collective properties.[1-4] Recently, special attention has been paid to spacings in the sub-nanometre range due to heightened expectations of their ultimate coupling, field enhancement, and even quantum effect.[5-9] However, so far, control of the inter-particle spacing at the sub-nanometre scale remains a challenge. For top-down technology, the sub-nanometre scale lies beyond the limitations of current lithography, so the location of nanoparticles within this range is beyond control. For bottom-up methods *i.e.* nanoparticle self-assembly, it was theoretically plausible as long as the length of the ligand of the nanoparticles was sufficiently short. Unfortunately, self-assembly of nanoparticles into an array is a delicate process, which requires the ligand to be long enough to provide the necessary repulsive force and spatial coherence to balance the inter-nanoparticle attractive force.[10-14] Therefore, self-assembly of nanoparticles into an array with sub-nanometre spacing is rarely reported.[15] The current published studies concerning sub-nanometre spacing are mainly based on selective individual pairs, and not the entire array.[16, 17]

It is well-known that nanoparticle self-assembly structures generally correspond to a meta-stable state, where the ligands and the nanoparticles are far from the compact arrangement. There is still vacant space left between the nanoparticles. The thermodynamic equilibrium state of the array should correspond to the close packing of nanoparticles with the most favorable arrangement of ligands. Unfortunately, such structure is difficult to obtain at room temperature, where the mobility of the ligands is too low to relax to the most favorable configuration efficiently. However, increasing temperature would make a difference. Suitably high temperature could offer the ligands enough mobility, which would allow the molecules to relax to the equilibrium state through filling the vacancy and further induce close packing of the nanoparticles. Therefore, thermal annealing of the prepared self-assembly nanoparticle array could be a possible solution to reduce the distance between nanoparticles and achieve the control of sub-nanometre spacing.

Based on the above consideration, an Au nanoparticle (Au NP) array was used as a model to explore its behaviour under thermal annealing. TEM and 2D grazing incidence small angle X-ray scattering (GISAXS)[18] demonstrated that thermal annealing could decrease the inter-particle spacing. Quantitative measurement of the spacing by 1D GISAXS indicated that the spacing in the array gradually changed from its original value of 1.68 nm to as low as 0.57 nm as the annealing process progressed. In addition, the molecular dynamics simulation verified that the spacing decrease corresponded to the relaxation of the array to the thermodynamic equilibrium structure as expected. All of these results proved that relaxation of the nanoparticle array by thermal annealing was an effective way to adjust the inter-particle spacing at the nanometre scale.

The Au NP array was fabricated according to published methods.[19, 20] Firstly the Au NPs (diameter of 5.90 ± 1.31 nm, UV-vis absorption peak at 518 nm, Figure S1) were synthesised by reduction of $HAuCl_4$ with $NaBH_4$ in water, followed by their transfer into hexane using 1-dodecanethiol (DDT). Then the alkyl chain passivated nanoparticles were self-assembled on the surface of a toluene droplet and deposited on a Teflon™ substrate after the toluene had evaporated. As shown in Figure 1(A), in the array the nanoparticles were arranged in a hexagonal structure. The distance between the centres of the adjacent nanoparticles was estimated at 7.44 ± 0.21 nm according to the fast Fourier transform (FFT) pattern, meaning that the inter-particle spacing was approximately 1.54 nm.

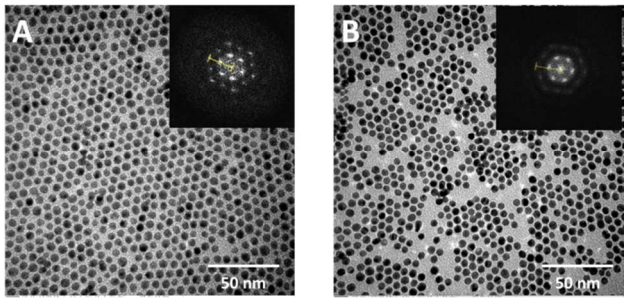

Figure 1 TEM images of the Au NP arrays before (A) and after 2 h thermal annealing (B). The inserts are the corresponding FFT patterns.

Thermal annealing of the prepared Au NP array was carried out in a vacuum oven at 80 ± 1 °C and at a pressure of 70 ± 5 Pa. Figure 1(B) shows the TEM image of the array after 2 h annealing. After thermal annealing, the Au NPs were packed much more closely than in the original. Meanwhile, the Au NPs shrank into domains as a result of their closer packing. FFT calculation further verified that the inter-particle spacing was reduced to ~0.50 nm. Furthermore, the Au NPs arrays before and after annealing, were characterised by the 2D GISAXS as shown in Figure 2. In the GISAXS patterns there were only two obvious diffraction arcs in the in-plane direction, which demonstrated that the gold nanoparticles formed an ordered structure parallel to the substrate. The positions of the arcs corresponded to the distance between the Au NPs. After annealing, the arcs became vague and meanwhile were shifted towards larger value in the *q*-direction, which indicated a reduction in their degree of ordering and in the distance between the nanoparticles. All of these results were in agreement with the TEM observations.

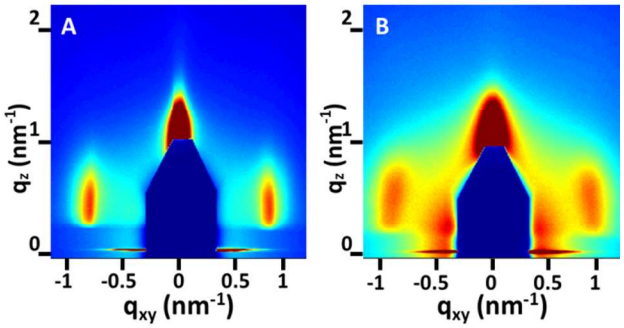

Figure 2 Two-dimensional GISAXS patterns of the Au NP arrays before (A) and after 2 h thermal annealing (B).

To quantitatively investigate the variation of the inter-particle spacing under thermal annealing, 1D, in-plane, GISAXS was used to characterize arrays annealed for different times. Figure 3 shows five representative curves, where the scattering peaks corresponded to the distance between the nanoparticles. In agreement with the 2D GISAXS, the peaks shifted to larger *q* values and their intensity declined with increasing annealing time due to the decrease of the distance and the degree of ordering. Based on the 1D GISAXS results, the variation of the spacing with annealing time is shown in the insert of Figure 3. The inter-particle spacing gradually decreased from 1.58 to 0.57 nm during the first 2 h of annealing and then maintained constant. This agreed with TEM observations, proving that an inter-particle spacing at sub-nanometre scale had been obtained. In addition, it indicated that the spacing could be continuously regulated by altering the annealing time.

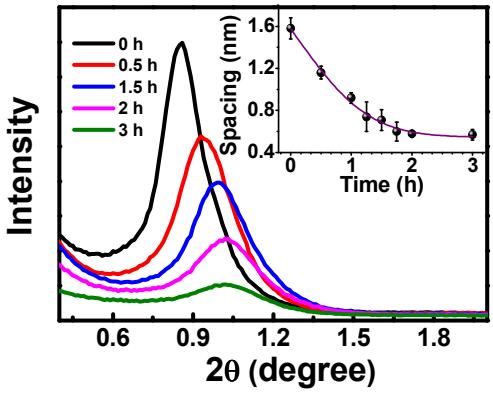

Figure 3 One-dimensional GISAXS curves of the Au NP arrays with 0, 0.5, 1, 2 and 3 h annealing time. The insert shows a plot of the inter-particle spacing *versus* the annealing time.

As is known, the inter-particle spacing variation would lead to a change in the Au nanoparticle surface plasma resonance (SPR) due to near-field coupling. Therefore arrays annealed for different times were monitored by UV-vis spectroscopy. As shown in Figure 4, the SPR wavelength of the Au nanoparticles in those arrays red-shifted from 557 ± 4 nm to 592 ± 2 nm with annealing time as expected. The relationship of the SPR wavelength and the spacing was analysed as shown in the insert of Figure 4. The SPR wavelength decayed almost exponentially with the inter-particle spacing. The decay could be well fitted to the plasmon ruler equation in the form:

$$\Delta\lambda/\lambda_0 = a \cdot \exp(-(s/D)/\tau) \quad (1)$$

(where *s* is the inter-particle spacing, *D* is the nanoparticle diameter, $\Delta\lambda$ is the shift of the SPR wavelength, λ_0 is the SPR wavelength of the pristine array, τ is the decay constant, and a is the amplitude).[21, 22] The estimated values of τ and a (from 5 sets of Au NP arrays) were 0.30 ± 0.04 and 0.18 ± 0.01 respectively, which agreed with published data.[21, 22]

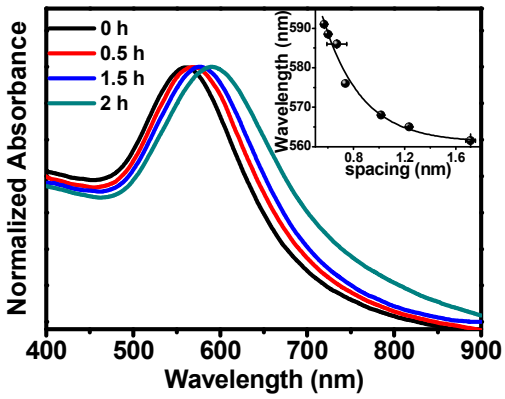

Figure 4. UV-vis spectra of the Au NP arrays with 0, 0.5, 1, and 2 h annealing time (The UV-vis spectra were measured after the samples were cooled to room temperature, not in-situ.). The insert shows a representative plot of the SPR wavelength *versus* the inter-particle spacing of one set of Au nanoparticle arrays.

To explain the spacing decrease, a molecular dynamics simulation model was established based upon the particle size measured experimentally and published surface grafting density data:[23, 24] this

helped to analyse the dependence of inter-nanoparticle energy E_{NP} upon the distance between nanoparticles. As shown in Figure S3, E_{NP} non-monotonically changed with the distance between nanoparticles. The lowest E_{NP}, signalling a thermodynamically stable packing between NPs, corresponded to a centre of mass distance between NPs of approximately 6.3 nm, which was close to the experimental values (6.40 nm in TEM, 6.47 nm in 1D GISAXS). Smaller distance could enhance the potential, which was in agreement with the above phenomenon that the spacing decrease with time had a limiting value. This simulation result proved that, with suitable annealing, the spacing between nanoparticles can be tuned to a value corresponding to a structure in thermodynamic equilibrium. For the ligand of DDT, the decrease of spacing is a process of condense packing, as shown in Scheme 1. Before annealing the DDT molecules were in a loose arrangement, leaving certain vacant space between nanoparticles. Thermal annealing enhanced the mobility of DDT molecules and promoted them to pack more and more closely until the space between nanoparticles was fully occupied.

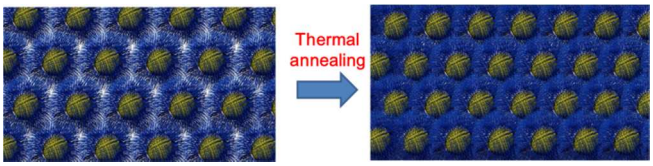

Scheme 1 Schematic presentation of the variation of the Au NP array under thermal annealing.

It is worth mentioning that the desorption of the ligand under high temperature also could cause the morphology change of nanoparticle arrays.[25] However, X-ray photoelectron spectroscopy (XPS) analysis indicated that the ratio of Au to S atoms in the array didn't show any remarkable change after 2 h annealing. This suggested that the ligand of DDT didn't loss under the annealing condition, thereby excluding the possibility that the DDT desorption resulted in the spacing decrease.

The temperature and pressure applied during thermal annealing influenced the spacing variation: an increased temperature would cause nanoparticle sintering. When the annealing temperature was 90 °C, the Au NPs sintered from time to time and no reliable variation in the process was obtained. The sintering could have been induced by the loss of the ligand. A decreased temperature would slow the process. When the temperature was 70 °C and the pressure was still 70 Pa, it took over 12 h to decrease the inter-particle spacing to 0.6 nm. An increased pressure would also slow the process: when the pressure increased to 2000 Pa, the spacing variation was almost unobservable. Both a decreased temperature and an increased pressure tended to depress the mobility of the molecules: therefore retarding the relaxation of the array as would have been expected intuitively. This analysis indicated that an ideal temperature, a low pressure, and sufficient annealing time were prerequisites for achieving sub-nanometre spacings. The difficulty therein may have accounted for the fact that, although thermal annealing of nanoparticle arrays has been explored, sub-nanometre spacing has not yet been reported before.[25, 26]

Conclusions

In summary, suitable thermal annealing could decrease the inter-particle spacing of a self-assembly array and allow the spacing to be adjusted at the sub-nanometre scale. This had the potential to significantly strengthen array function, and promised an ability to fabricate powerful devices therewith.

This work was supported by National Natural Science Foundation of China (21174024), National Science Foundation for Distinguished Young Scholars of China (21025416), Supporting Projects for Talents in the Universities of Liaoning Province (LR2012008) and Fundamental Research Funds for the Central Universities (N120505005, N120405007, N130305002, N130205001).

Notes and references

[a] College of Sciences, Northeastern University, Shenyang 110819, China
[b] State Key Laboratory of Theoretical and Computational Chemistry, Institute of Theoretical Chemistry, Jilin University, Changchun 130023, China
[c] State Key Lab of Polymer Physics and Chemistry, Changchun Institute of Applied Chemistry, Chinese Academy of Science, Changchun 130022, China
[d] College of Chemistry, State Key Laboratory of Supramolecular Structure and Materials, Jilin University, Changchun 130012, China

† Footnotes should appear here. These might include comments relevant to but not central to the matter under discussion, limited experimental and spectral data, and crystallographic data.

Electronic Supplementary Information (ESI) available: Materials and instruments, preparation of Au NPs and Au NPs array, thermal annealing, UV-Vis spectroscopy substrate prepara-tion, TEM sample preparation, GISAXS characterization, Simula-tion model and method and figures (S1−S3). See DOI: 10.1039/c000000x/

1. C.-F. Chen, S.-D. Tzeng, H.-Y. Chen, K.-J. Lin and S. Gwo, *J. Am. Chem. Soc.*, 2007, **130**, 824-826.
2. M.-H. Lin, H.-Y. Chen and S. Gwo, *J. Am. Chem. Soc.*, 2010, **132**, 11259-11263.
3. C. T. Black, C. B. Murray, R. L. Sandstrom and S. Sun, *Science* 2000, **290**, 1131-1134.
4. W. L. Cheng, M. J. Campolongo, J. J. Cha, S. J. Tan, C. C. Umbach, D. A. Muller and D. Luo, *Nat. Mater.*, 2009, **8**, 519-525.
5. R. Esteban, A. G. Borisov, P. Nordlander and J. Aizpurua, *Nat. Commun.*, 2012, **3**, 825-834.
6. K. J. Savage, M. M. Hawkeye, R. Esteban, A. G. Borisov, J. Aizpurua and J. J. Baumberg, *Nature*, 2012, **491**, 574-577.
7. E. C. Le Ru, P. G. Etchegoin and M. Meyer, *J. Chem. Phys.*, 2006, **125**, 204701.
8. J.-H. Lee, J.-M. Nam, K.-S. Jeon, D.-K. Lim, H. Kim, S. Kwon, H. Lee and Y. D. Suh, *ACS Nano*, 2012, **6**, 9574-9584.
9. J. Zuloaga, E. Prodan and P. Nordlander, *Nano Lett.*, 2009, **9**, 887-891.
10. D. Vanmaekelbergh, *Nano Today*, 2011, **6**, 419-437.
11. B. L. V. Prasad, C. M. Sorensen and K. J. Klabunde, *Chem. Soc. Rev.*, 2008, **37**, 1871-1883.
12. H. Ma and J. Hao, *Chem. Soc. Rev.*, 2011, **40**, 5457-5471.
13. J. Gong, G. Li and Z. Tang, *Nano Today*, 2012, **7**, 564-585.
14. K. C. Ng, I. B. Udagedara, I. D. Rukhlenko, Y. Chen, Y. Tang, M. Premaratne and W. L. Cheng, *Acs Nano*, 2012, **6**, 925-934.
15. C. P. Collier, R. J. Saykally, J. J. Shiang, S. E. Henrichs and J. R. Heath, *Science*, 1997, **277**, 1978-1981.
16. J. Kern, S. Grossmann, N. V. Tarakina, T. Hackel, M. Emmerling, M. Kamp, J. S. Huang, P. Biagioni, J. C. Prangsma and B. Hecht, *Nano Lett.*, 2012, **12**, 5504-5509.
17. H. Duan, A. I. Fernández-Domínguez, M. Bosman, S. A. Maier and J. K. W. Yang, *Nano Lett.*, 2012, **12**, 1683-1689.
18. M. J. Campolongo, S. J. Tan, D. M. Smilgies, M. Zhao, Y. Chen, I. Xhangolli, W. L. Cheng and D. Luo, *Acs Nano*, 2011, **5**, 7978-7985.
19. M. N. Martin, J. I. Basham, P. Chando and S.-K. Eah, *Langmuir*, 2010, **26**, 7410-7417.

20. J. Zhou, J. Ni, Y. Song, B. Chen, Y. Li, Y. Zhang, F. Li, Y. Jiao and Y. Fu, *J. Mater. Chem. C*, 2014, **2**, 6410–6414.
21. P. K. Jain, W. Huang and M. A. El-Sayed, *Nano Lett.*, 2007, **7**, 2080-2088.
22. K. H. Su, Q. H. Wei, X. Zhang, J. J. Mock, D. R. Smith and S. Schultz, *Nano Lett.*, 2003, **3**, 1087-1090.
23. D. V. Leff, P. C. Ohara, J. R. Heath and W. M. Gelbart, *J. Phys. Chem.* , 1995, **99**, 7036-7041.
24. H. Sellers, A. Ulman, Y. Shnidman and J. E. Eilers, *J. Am. Chem. Soc.*, 1993, **115**, 9389-9401.
25. I. Robel, X. M. Lin, M. Sprung and J. Wang, *J. Phys.: Condens. Matter*, 2009, **21**, 264011.
26. J. Luo, M. M. Maye, L. Han, N. N. Kariuki, V. W. Jones, Y. Lin, M. H. Engelhard and C.-J. Zhong, *Langmuir*, 2004, **20**, 4254-4260.

